

Travelling waves in arrays of delay-coupled phase oscillators

Carlo R. Laing*

*Institute of Natural and Mathematical Sciences, Massey University,
Private Bag 102-904 NSMC, Auckland, New Zealand*

In both networks we assume that the oscillators are heterogeneous. The effects of delays on the dynamics of coupled oscillator networks have been considered a number of times previously [10, 15, 24, 52, 55], but here we will extensively use the recent ansatz of Ott and Antonsen [46, 47] to derive continuum level descriptions of travelling waves, which will make the formulation of delayed equations straightforward.

We study Kuramoto oscillators in Sec. II and theta neurons in Sec. III. For the Kuramoto oscillators we consider constant delays in Sec. II B, transmission delays in Sec. II C and distributed

where

$$G(x) = \begin{cases} \frac{1}{4}, & |x| < 2 \\ 0, & \text{otherwise} \end{cases} \quad (6)$$

and the spatial integral is evaluated using periodic boundary conditions. The density f satisfies the continuity equation

$$-\frac{f}{t} + \nabla \cdot (fv) = 0 \quad (7)$$

where

$$v = \frac{K}{2i} Z e^{-i} - \bar{Z} e^i \quad (8)$$

The system (7)-(8) is amenable to the Ott/Antonsen ansatz [46, 47] so we write

$$f(x, y, x, t) = \frac{g(\cdot)}{2} \left[1 + \sum_{n=1}^{\infty} \{\bar{z}(\cdot, x, t)\}^n e^{in} + \text{c.c.} \right] \quad (9)$$

for some function $z(\cdot, x, t)$ where "c.c." is the complex conjugate of the previous term. This ansatz is an assumption that f takes the particular form (9). Substituting (9) into (5) and (7)-(8) we find that z satisfies

$$-\frac{z}{t} = i z + \frac{K}{2} Z - \bar{Z} z^2 \quad (10)$$

where

$$Z(x, t) = \int_0^2 G(x-y) \int_{-\infty}^{\infty} g(\cdot) z(\cdot, y, t) dy \quad (11)$$

Using contour integration to evaluate the integral over \cdot in (11) and defining $u(x, t) = z(\cdot - i, x, t)$ we find that u satisfies

$$-\frac{u}{t} = (-1 + i \cdot_0) u + \frac{K}{2} Z - \bar{Z} u^2 \quad (12)$$

where

$$Z(x, t) = \int_0^2 G(x-y) u(y, t) dy \quad (13)$$

Partially coherent uniformly-twisted states are solutions of (12)-(13) of the form $u(x, t) = a e^{i(qx + \cdot t)}$ where a and \cdot are real and q is an integer (the "twist" of a twisted state; an integer because of the periodic boundary conditions of the domain). The quantity a ($0 < a < 1$) measures the coherence level of a state: a increases as the coherence increases, q gives the rate at which the phase of u changes with x at a fixed t , while \cdot gives the temporal rotation rate of a twisted state. Substituting this form of solution into (12)-(13) we find

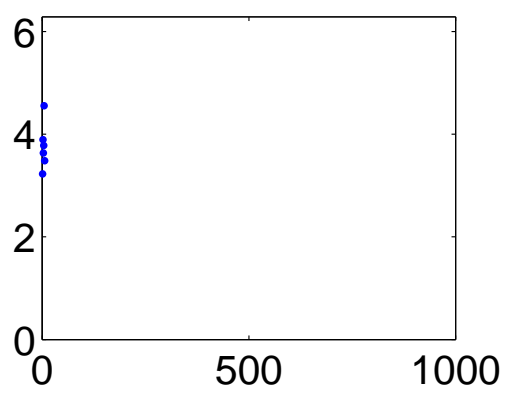
$$i \cdot = -1 + i \cdot_0 + \frac{KG(q)}{2} (1 - a^2) \quad (14)$$

where G is the Fourier transform of G :

$$G(q) = \int_0^2 G(x) \cos(qx) dx = \frac{\sin(2 \cdot q)}{2 \cdot q} \quad (15)$$

for the coupling function given by (6). Equating real and imaginary parts of (14) we find

$$a^2 = 1 - \frac{2}{KG(q)} \quad \text{and} \quad \cdot = \cdot_0 \quad (16)$$



and $|x - y|$ denotes the shortest distance between points x and y on the circle, i.e. $|x - y| = \min(|x - y|, 2\pi - |x - y|)$. For a twisted state $u(x, t) = ae^{i(qx + t)}$ and coupling function (6)

$$Z(x, t) = \frac{iae^{i(qx + t)}}{4} \frac{1 - e^{2i(q - s)}}{q - s} - \frac{1 - e^{-2i(q + s)}}{q + s} \quad (29)$$

and thus twisted states are solutions of

$$i = -1 + i_0 + \frac{K}{2} - a^2 \quad (30)$$

where

$$\equiv \frac{i}{4} \frac{1 - e^{2i(q - s)}}{q - s} - \frac{1 - e^{-2i(q + s)}}{q + s} \quad (31)$$

Setting $a = 0$ we find that for fixed i and s a q -twisted state is created at

$$K = \frac{2}{\text{Re}(\cdot)} \quad (32)$$

where \cdot is a solution of

$$= i_0 + \frac{\text{Im}(\cdot)}{\text{Re}(\cdot)} \quad (33)$$

We know that for $s = 0$, $\text{Im}(\cdot) = 0$ and thus $\cdot = i_0$ and a q -twisted state is created at $K = 2/G(q)$. Following these bifurcations as s is increased from zero we obtain the curves shown with solid lines in Fig. 4. The stability of these solutions was found by direct simulation to change via a Hopf bifurcation at the points indicated by circles in Fig. 4. We see that for these parameter values, increasing s , i.e. decreasing the transmission velocity, moves all curves to higher values of K .

We finish this section by noting that when performing the reduction of general weakly coupled oscillators with transmission delay to phase oscillators, the delay appears as a phase shift, i.e. one obtains an undelayed system of the form

$$\frac{d_j}{dt} = j + \frac{K}{2M + 1} \sum_{k=-M}^M \sin(j_{+k} - j - |k| x) \quad (34)$$

where \cdot is a constant [7, 15]. We will not consider such a system here.

D. Distributed delay

We now consider distributed delays. Let us define the complex mean field as in (3) but then suppose that oscillator j is influenced by a delayed version of Z_j , as in [31, 39], i.e. define

$$R_j(t) = \int_0^\infty Z_j(t - \tau) h(\tau) d\tau \quad (35)$$

where $h(\tau)$ is the probability density of the delay τ , and let the oscillator dynamics be

$$\frac{d_j}{dt} = j + K \text{Im} R_j e^{-i j} = j + \frac{K}{2i} R_j e^{-i j} - \bar{R}_j e^{i j} \quad (36)$$

(As presented, we calculate $R_j(t)$ by first forming the local mean field and then delaying it. Since the sum in (3) and the integral in (35) commute we can also think of $R_j(t)$ as resulting from first delaying all the z_j s and then forming the local mean field from those delayed values.) Moving to the continuum limit and performing the integrals as above we obtain

$$\frac{u(x, t)}{t} = (-1 + i_0)u(x, t) + \frac{K}{2} R(x, t) - \bar{R}(x, t)u^2(x, t) \quad (37)$$

Setting $a = 0$ we find that a q -twisted state is created at

$$K = \frac{2}{G(q)} \left[1 + \frac{2}{(1 + \frac{2}{q})^2} \right] \quad (43)$$

Instead of varying q we will set $q = 2$ and vary ω_0 , as doing so leads to some interesting behaviour [31, 39]. As in Sec. II B we move to a rotating coordinate frame at speed ω_0 , i.e. let $\tilde{u}(x, t) = u(x, t)e^{-i\omega_0 t}$, $\tilde{R}(x, t) = R(x, t)e^{-i\omega_0 t}$ and $\tilde{Z}(x, t) = Z(x, t)e^{-i\omega_0 t}$ so that \tilde{u} is a fixed point of

$$\frac{\partial \tilde{u}(x, t)}{\partial t} = (-1 + i(\omega_0 - \frac{1}{2}))\tilde{u}(x, t) + \frac{K}{2} \tilde{R}(x, t) - \tilde{R}(x, t)\tilde{u}^2(x, t) \quad (44)$$

where

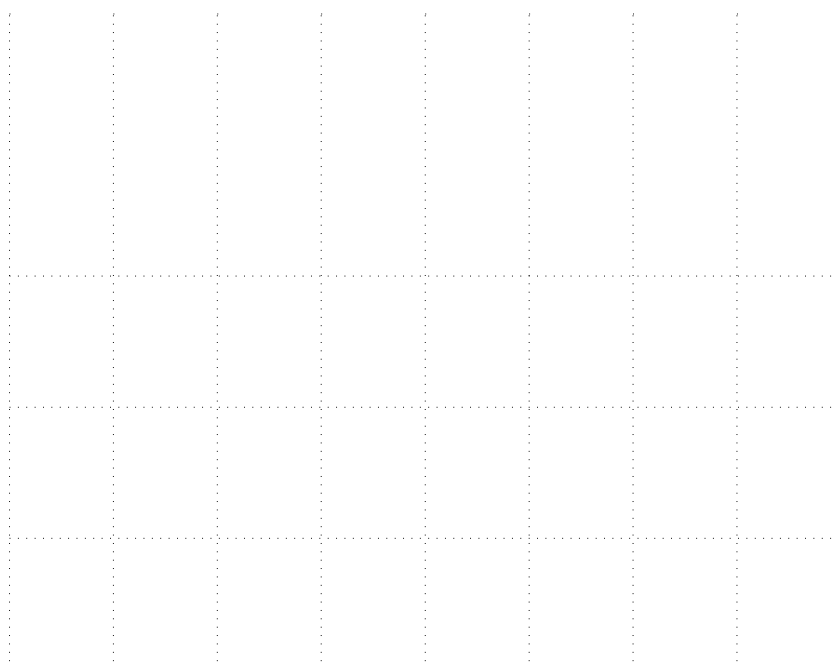
$$\frac{\partial \tilde{R}(x, t)}{\partial t} = \tilde{Z}(x, t) - \tilde{R}(x, t) - i \tilde{R}(x, t) \quad (45)$$

and

$$\tilde{Z}(x, t) = \int_0^2 G(x - y)\tilde{u}(y, t)dy \quad (46)$$

Following bifurcations of twisted states we obtain the results in Fig. 5. For ω_0 small we obtain similar results to previous sections, but for larger ω_0 we see that twisted states are created in saddle-node bifurcations as K is increased. In this range the bifurcation from the zero state is subcritical, leading to the creation of an unstable branch which is stabilised through either a saddle-node bifurcation (for $q = 0$) or in a Hopf bifurcation (for $q > 0$).

Figure 6 shows a plot of a versus K for $\omega_0 = 2.5$, i.e. at the right edge of Fig. 5. Recalling that the zero state is stable for $K < 2[1 + (\frac{2}{\omega_0/(1 + \frac{2}{q})})^2]$ (68/9 for the parameters used here)



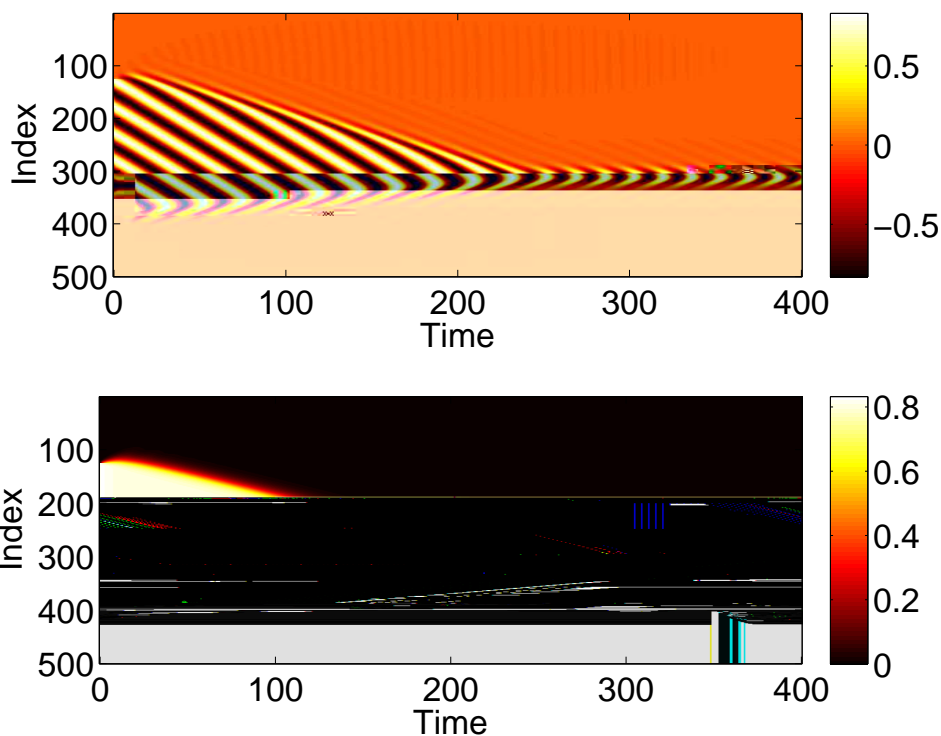


FIG. 8: Solutions of (37)-(38). Top: $\text{Re}(u)$; bottom: $|u|$, shown color-coded. Parameters as in Fig. 7.

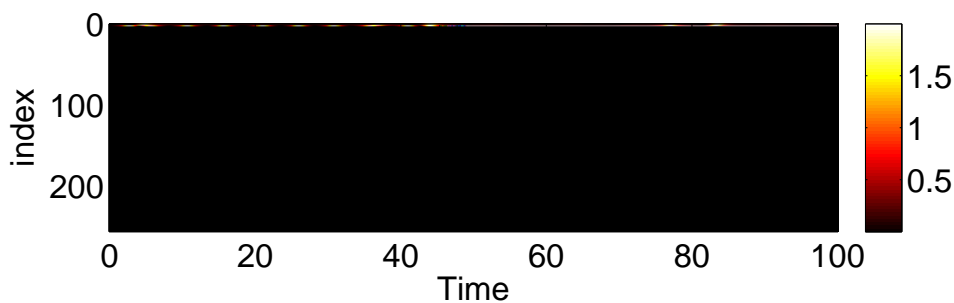
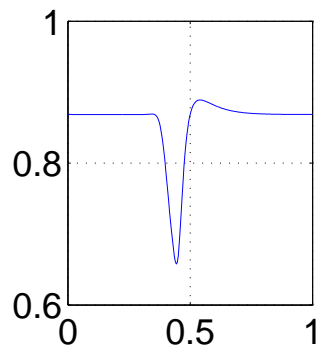
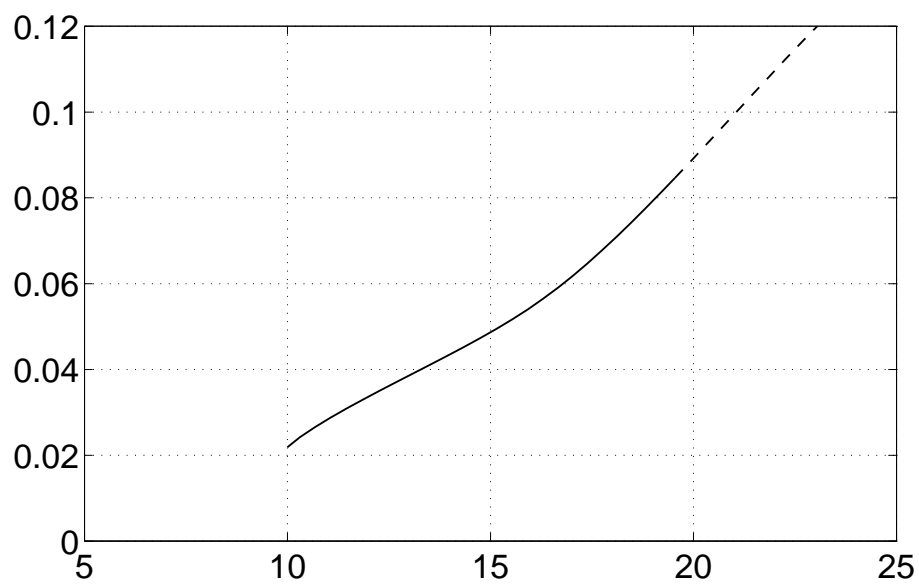


FIG. 9: Travelling wave solution of (47)-(48). $1 - \cos \theta$ is shown in colour. Parameters: $N = 256$, $M = 16$, $I_0 = -0.2$, $\tau = 0.05$, $g = 11$, $n = 2$.

shown in Fig. 10. These pulses move with a fixed profile at a constant speed. Note that the argument of z increases through 2π once as we move around the domain, and this point corresponds to the maximum of the firing frequency, as expected. (The network also supports travelling pulses with





2011.
[40] Tanushree B Luke, Ernest Barreto, and Paul So. Complete classification of the macroscopic behavior